ISSN 1392-3196 / e-ISSN 2335-8947
Zemdirbyste-Agriculture, vol. 101, No. 4 (2014), p. 453−460
DOI 10.13080/z-a.2014.101.058

Comparative proteomic analysis of pollen of *Trifolium pratense*, *T. alexandrinum* and *T. repens*

Gražina TREIGYTĖ[1], Ilona ZAIKOVA[1], Dalius MATUZEVIČIUS[2], Violeta ČEKSTERYTĖ[3], Giedrė DABKEVIČIENĖ[3], Bogumila KURTINAITIENĖ[1], Rūta NAVAKAUSKIENĖ[1]

[1]Institute of Biochemistry, Vilnius University
Mokslininkų 12, Vilnius, Lithuania
E-mail: ruta.navakauskiene@bchi.vu.lt

[2]Vilnius Gediminas Technical University
Naugarduko 41-422, Vilnius, Lithuania

[3]Institute of Agriculture, Lithuanian Research Centre for Agriculture and Forestry
Instituto 1, Akademija, Kėdainiai distr., Lithuania

Abstract

Clovers are widely distributed, but their pollen proteome still has not been completely elucidated. In this study we performed a comprehensive comparative proteomic analysis of red, berseem and white clover pollen. Hand-collected pollen of different clover species were used for total protein extraction. Proteins isolated from red clover cvs. 'Kiršiniai' and 'Vyčiai', berseem clover cv. 'Faraon' and white clover cv. 'Medūnai', populations Nos. 2295 4n and 2196 4n, were subjected to fractionation by one-dimensional electrophoresis. Some quantitatively different protein groups were characterized in protein maps typical of analyzed clover pollens. For the detailed proteomic analysis we chose pollen of red clover cv. 'Vyčiai', berseem clover cv. 'Faraon' and white clover cv. 'Medūnai'. Proteins isolated from the pollen were fractionated by two-dimensional electrophoresis (2DE) and stained for visualisation by using Coomassie blue. Each of the 2DE images indicated over 200 protein spots. Computational methods developed by us were applied for characterization and comparison of proteins isolated from the pollen of the three clover species. The computational methods enabled the evaluation of protein expression variations in red, berseem and white clover pollen proteome maps. By using computer-assisted image analysis of the gels, the expression levels of the proteins were evaluated and their molecular weight and isoelectric point were precisely characterized. We detected over 30 protein spots whose quantitative levels were most divergent in investigated clover pollen proteome map. They were analyzed by mass spectrometry and identified. The fold changes of identified proteins representing red clover cv. 'Vyčiai', berseem clover cv. 'Faraon' and white clover cv. 'Medūnai' were calculated using computer-assisted methods.

Key words: berseem clover, pollen, proteomic analysis, red clover, white clover.

Introduction

The pollen proteome characteristic of different plant species may vary significantly. The proteomic specificity of pollen can influence the preference of the honeybee and the quality of honey. Therefore it is important to perform a comprehensive analysis of proteomes characteristic of pollen specific to different clover species.

Clovers, like most legumes, are co-evolved complexes of plant, symbiotic bacteria, fungi, and insect pollinators (Vilčinskas, Dabkevičienė, 2009; Williams, Nichols, 2011). The clover genus *Trifolium* has over 200 species (Ellison et al., 2006; Badr et al., 2008), about 10% of which are used as forage plants in commercial agriculture, and a greater number are used locally for fodder (Williams, Nichols, 2011). The most important clover species are white clover (*Trifolium repens* L.), red clover (*Trifolium pratense* L.) and berseem clover (*Trifolium alexandrinum* L.). Berseem clover is widely cultivated as a forage crop in Asia and Africa. The varieties of genetic improvements of the crop that had been developed in Egypt were later distributed worldwide (Badr et al., 2008). White clover (*T. repens* L.) is a temperate perennial forage legume widely used in pastoral systems. White clover progenitors are putatively identified as the diploid species. The white clover genome is moderately compact (Griffiths et al., 2013). Proteomic analysis of senescence, a final step of leaf development, was carried out in white clover *T. repens*. Wilson and co-workers (2002) performed a quantitative analysis of 590 leaf protein spots separated by two-dimensional electrophoresis and indicated that approximately 40% of the spots (178 spots) showed significant senescence related changes in abundance. Red clover is a species, native to Europe, but planted in many other regions. It is considered that red clover is one of the richest sources of isoflavones. It was found that honey bees could

be excellent foragers in red clover fields, foraging an average of 98.4% of the time during peak bloom on the target crop (Jevtic et al., 2013).

In our study we presented a comprehensive proteomic analysis of pollen of three most important clover species – red clover (*Trifolium pratense* L.), berseem clover (*Trifolium alexandrinum* L.) and white clover (*Trifolium repens* L.).

Materials and methods

Clover species: red clover cvs. 'Kiršiniai' and 'Vyčiai', berseem clover cv. 'Faraon' and white clover cv. 'Medūnai', and populations No. 2295 4n and No. 2196 4n were used for pollen production. The clover species were grown in the greenhouse of the Laboratory of Genetics and Physiology, Institute of Agriculture, Lithuanian Research Centre for Agriculture and Forestry in 2013 under controlled conditions (at 18–24°C temperature, 16 h photoperiod). The plants started flowering in April.

Collection of pollen. For pollen collection, flowers were picked from red clover cvs. 'Kiršiniai' and 'Vyčiai', berseem clover cv. 'Faraon' and white clover cv. 'Medūnai', and populations No. 2295 4n and No. 2196 4n. Pollen grains were manually collected into Eppendorf tubes (Eppendorf AG, Germany) and immediately placed in a storage at −80°C until analysis.

Protein isolation from pollen. Proteins from mature pollen (aprox. 20 mg) were isolated as described by Sheoran and co-workers (2009). Shortly, mature pollen was homogenized with acetone containing 10% trichloroacetic acid (TCA) and 1% dithiothreitol (DTT). The solution was centrifuged 20.000 × g for 20 min at 4°C and pellet was washed two more times with acetone solution containing 1% DTT. The pellet was dried in vacuum and proteins were extracted with isoelectric focusing (IEF) lysis buffer containing 9 M urea, 2 M thiourea, 4% CHAPS (3-[(3-Cholamidopropyl) dimethylammonio]-1- propanesulfonate), 1% DTT, 0.8% IPG (immobiline pH gradient) buffer, pH 3–10. The solution was centrifuged 20.000 × g for 20 min at 4°C and pellet was extracted again with IEF lysis buffer. After centrifugation, both extracts were combined and directly used for protein analysis or stored at −20°C until analysis.

Gel electrophoresis. The pollen proteins were resolved by sodium dodecyl sulphate-polyacrylamide gel electrophoresis (SDS/PAGE) and two-dimensional gel electrophoresis (IEF/SDS). For the former technique, we used 8–16% polyacrylamide gradient gel (ICN Biomedicals Inc., Sweden) in tris-glycine electrophoresis buffer. For two-dimensional electrophoresis (2DE) an Immobiline DryStrip kit, pH range 3–10 and *Excel* gel SDS, gradient 8–18% was used. It was carried out according to the manufacturer's instructions (Immobiline DryStrip kit for 2DE with Immobiline DryStrip and Excel gel SDS, Pharmacia Biotech, Sweden). For protein visualization gels were stained with colloidal Coomassie G-250 (Bio-Rad Laboratories, USA). For 2DE fractionation of pollen proteins three independent biological experiments were carried out. Images of representative 2DE fractionation are shown in Figures 1 and 2.

In-gel digestion and MALDI-TOF MS. Areas of interest were cut out from the 2DE gels and subjected to overnight in-gel tryptic digestion (Shevchenko et al., 1996). Briefly, the gel slices were dehydrated with 50% acetonitrile and then dried completely using a centrifugal evaporator DNA Mini (Eppendorf AG). The protein spot was rehydrated in 30 µl of 25 mM ammonium bicarbonate (pH 8.3) containing 25 µg ml^{-1} modified trypsin (Promega, USA), and the samples were incubated overnight at 37°C. The tryptic peptides were subsequently extracted from the gel slices as follows. Any extraneous solution remaining after the digestion was removed and placed in a fresh tube. The gel slices were washed twice with 5% trifluoracetic acid in 50% acetonitrile, shaking occasionally. The digestion and extract solutions were then combined and evaporated to dryness. For MALDI-TOF analysis, the peptides were dissolved in 3 µl of 30% acetonitrile and 0.01% trifluoracetic acid and were then prepared with a matrix (α-cyano-4-hydroxicinnamic acid) on the target plate. The analysis was performed on a 4800 MALDI TOF/TOF™ mass spectrometer (Applied Biosystems/ MDS SCIEX, Canada) and externally calibrated using synthetic peptides with known masses. MS reflector mode settings: m/z range 800–4000, mass accuracy ±50 ppm, MS/MS mode settings: collision energy 1 keV, CID – no CID used, fragment mass accuracy ±0.1 Da. The mass information generated from the composite spectrum was submitted to a search performed with the databases *UniProt* and *Expasy*. Results from three independent biological experiments are summarized in Table.

Image acquisition and data analysis. Stained 2DE gels were digitized on ImageScanner™ III scanner (GE Healthcare Biosciences, Germany) using software *LabScan 6.0* application that is specialized for acquisition of 2DE gel images. To ensure linearity of response and minimize software-induced variance in gel image analysis, calibration of the scanner is performed before scans using provided step tablet. Gels were scanned at 300 dpi resolution and saved in tiff. format. Analysis of 2DE gel images was performed using originally developed software prototype with new pre-processing, alignment, segmentation and subsequent analysis algorithms. All required tools were implemented using programming language Matlab™ (The MathWorks, USA). Employed software tools allow: to crop gel images in order to keep only protein separation area; align images; automatically detect protein spots; manually edit protein spot area to eliminate false positives and false negatives if needed; quantify spots and estimate expression changes; visualize gel regions in 3-D or 2-D. The process of 2DE gel image analysis can be performed in two basic ways: spot detection and delineation are performed prior to image alignment, or in the reversed order (Dowsey et al., 2010). Gel image analysis workflow used here is as follows: image pre-processing, image alignment, spot detection-segmentation in aligned images, and differential analysis. A more detailed explanation of the developed and applied algorithms is presented in the Discussion part.

Results and discussion

Quantitative analysis of the proteins corresponding to different species of red, berseem and white clover pollen. Pollen proteins were isolated from different clover species: red clover cvs. 'Kiršiniai' and 'Vyčiai', berseem clover cv. 'Faraon', white clover cv. 'Medūnai', populations Nos. 2295 4n and 2196 4n. Electrophoretic analysis of isolated proteins is presented in Figure 1. We determined some proteins groups those quantitative changes are most significant. These protein groups are detected in white clover cv. 'Medūnai' pollen (~20 kDa) and berseem clover cv. 'Faraon' pollen (~200, 105, 50, 15 and 13 kDa).

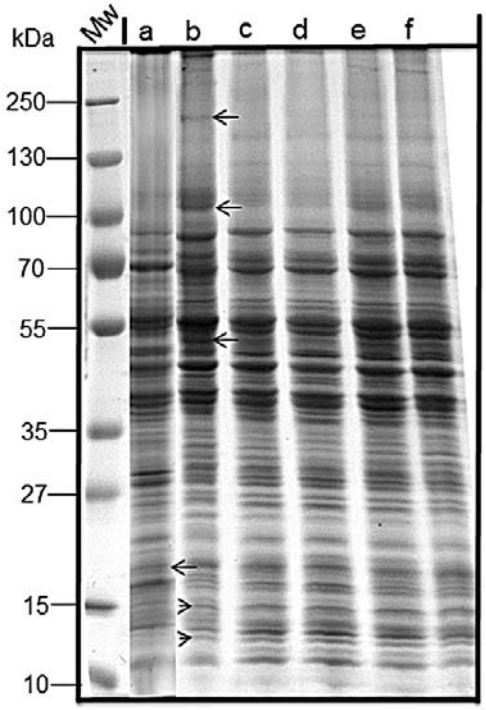

Notes. Proteins from different clover species were isolated as described in the section Materials and methods and fractionated in 8–16% polyacrylamide gradient gel in tris-glycine electrophoresis buffer and visualised by staining with colloidal Coomassie G-250. On the top of SDS/PAGE image clover species is indicated: a) white clover cv. 'Medūnai'; b) berseem clover cv. 'Faraon', c) red clover cv. 'Kiršiniai', d) red clover No. 2295 4n, e) red clover No. 2196 4n; f) red clover cv. 'Vyčiai'. Arrows indicate the protein groups whose quantitative changes are most significant. On the left side of the image the molecular weight is indicated. Representative images from one of three experiments showing similar results are shown.

Figure 1. Gel electrophoretic analysis of clover pollen proteins

2DE gel image analysis for differentially expressed proteins. Gel image analysis workflow used here is as follows: image pre-processing, image alignment, spot detection-segmentation in aligned images, and differential analysis. During the image pre-processing procedure, image cropping, noise reduction, and removal of background variations are carried out. The cropping of the gel images is used to exclude gel edges that are not useful for the image alignment. This improves alignment and reduces computation time. Noise reduction suppresses randomly occurring white and black pixels (impulse noise). Initial background subtraction is applied in order to compensate interfering variations in the gel background intensity level. Gradual change of background is corrected by the mathematical morphology approach. We used *Top-Hat* operation – subtraction of morphologically opened image from the original image – with disk-shaped structuring element. Gel image alignment and matching of protein spots is needed to enable quantitative comparison of spots from different 2DE gel images (Moller, Posch, 2009). Matching procedure usually requires defining landmarks that are common to both images. Thus the landmarks are the reference points used to guide warping of gel images. We designed image registration algorithm which initially detects strong landmarks between images, uses them for rigid deformation of images, then finds all correspondences between images, and finally computes elastic thin-plate spline transformation for the overlaid visualization of images and for pairing of the protein spots (Bookstein, 1989). During the initial alignment of 2DE gel images, algorithm distinguishes such matches between gel images which have the highest reliability (Matuzevicius, 2010). Initial alignment is based on a few key processes – finding image regions of interest (ROIs), similarity assessment between ROIs, establishment of matches, and error search. Method for detection of similar 2DE image regions is based on multi-layer perceptron combined with Lowe's key point descriptors (Lowe, 2004). Finally, in order to find all spot correspondences between images, similar strategy is used, only the search of similar regions is restricted to the smaller neighbourhoods of the spots. Results of automatic spot pairing, i.e. alignment vectors, may be reviewed and edited manually if correction of mismatches or additional pairings are needed.

Spot detection and segmentation is the next challenging stage in 2DE gel image analysis (Serackis, Navakauskas, 2010). The purpose of protein spot detection is to find probable positions of protein spots. Results of segmentation are spot boundaries that delineate spot area from background and other spots. Segmented spot area is used as ROI for spot volume calculations. Applied protein spot detection and segmentation algorithm is based on watershed transformation (WTS) combined with multiscale symmetrical feature detection. WTS in image analysis is useful for efficient image decomposition into such distinct areas that have only one regional minimum (Vincent, Soille, 1991). Dark protein spots in 2DE gel images are represented as pits of intensity, thus WTS is suitable for image decomposition when spots have to be separated. In order to ensure spot separation, to reduce over segmentation, which is common in image segmentation using WTS due to its sensitivity to image noise, and to enhance spot boundary determination, WTS is performed on feature maps, generated using differences of Gaussians algorithm. Filters designed using differences of Gaussians (DoG) algorithm are key elements in modelling of neural processing in the retina of the eye (Croner, Kaplan, 1995). Similarly to the eye, here DoG algorithm enhances important features of the gel image that guides WTS. Having results of image alignment and segmentation of the protein spots in gel images, a ratio of normalized spot quantities between the image groups can be calculated to estimate changes of spot abundance between the gel groups (Matuzevicius et al., 2008).

Results of accomplished quantitative 2DE gel (Fig. 2) image analysis are summarized in Table. Ratios of normalized spot quantities together with experimental molecular weight (MW) and isoelectric point (pI) were estimated. Proteins identified by using mass spectrometry analysis are marked with arrows in Figure 2.

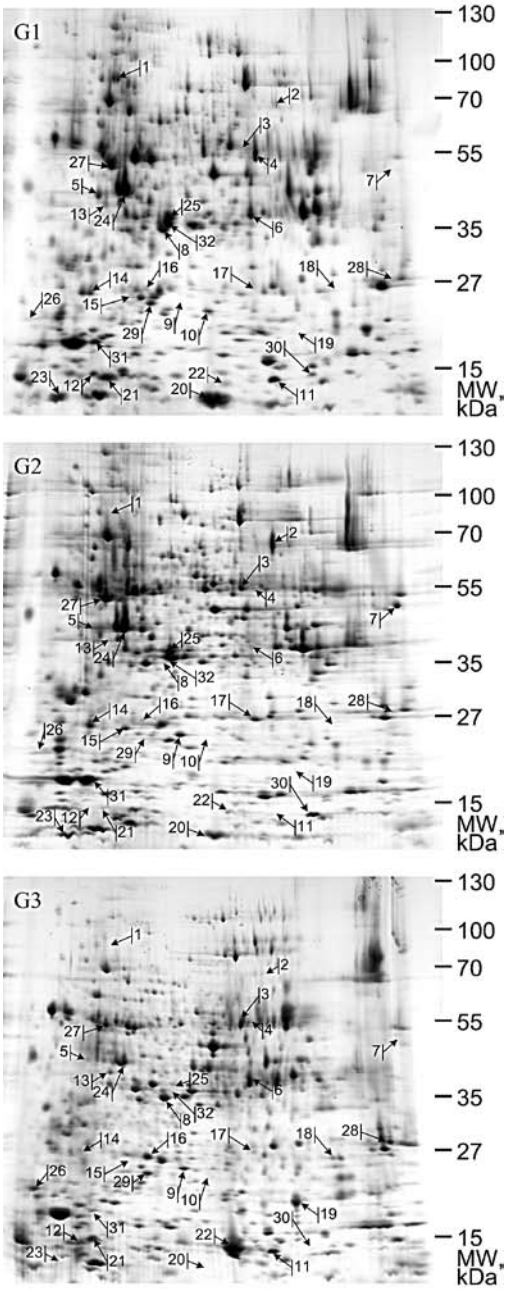

Notes. Proteins isolated from pollen of red clover cv. 'Vyčiai', berseem clover cv. 'Faraon', white clover cv. 'Medūnai' were separated with 2DE and stained with colloidal Coomassie G-250. For 2DE an Immobiline DryStrip kit, pH range 3–10 and *Excel* Gel SDS, gradient 8–18% were used. Protein maps represent total pollen proteins from red clover cv. 'Vyčiai' (G1), berseem clover cv. 'Faraon' (G2) and white clover cv. 'Medūnai' (G3). Arrows and numbers in the 2DE maps indicate the positions of proteins supplied to MALDI-TOF MS/MS and identified. Spot labels are the same as in Table. Representative images from one of the three experiments showing similar results are presented.

Figure 2. 2D gel electrophoretic maps of pollen proteins

Isoelectric points (pI) of identified proteins were calculated by interpolating between known pI values obtained from the standard pI 3–11 gel. Molecular weights (MWs) of polypeptide spots were computed using a standard procedure, i.e. MWs of proteins were determined by comparing their relative mobility with that of several marker proteins (standards) of a known molecular weight using a standard curve. Molecular weights were determined in all gels from the set before alignment procedure. Changes in spot volume were represented as ratios of averages of normalized spot volumes as described previously. An increase in spot abundance is represented with positive fold change and a decrease, with a negative fold change. Changes between protein spots from gels correspondent with protein maps of red clover cv. 'Vyčiai' (Fig. 2, G1), berseem clover cv. 'Faraon' (Fig. 2, G2) and white clover cv. 'Medūnai' (Fig. 2, G3) are summarized in Table.

Proteomic identification of differentially expressed proteins in clover pollen. For identification and analysis of pollen proteins they were isolated from red clover cv. 'Vyčiai', berseem clover cv. 'Faraon' and white clover cv. 'Medūnai', separated in 2DE system and stained with colloidal Coomassie G-250. Protein spots that were found to be most divergent in quantitative levels in different clover species were cut out and supplied to MALDI-TOF MS/MS analysis and identified. To our knowledge, the proteomic analysis of clover leaves is done by Wilson and co-workers (2002) and it shows that approximately 40% of identified protein spots are related to senescence changes. Chloroplast protein composition included certain proteins that indicate the importance of proteolysis, chloroplast degradation and remobilisation of nitrogen in leaf senescence (Wilson et al., 2002). Some other proteomic analyses were done on tobacco pollen (Fila et al., 2011), tomato pollen (Sheoran et al., 2007), maize pollen (Zhu et al., 2011) and others.

In the present study we identified more than 30 proteins whose quantitative levels differ in pollen of various clover species. We found that the identified proteins are involved in different cellular processes – structural and signalling proteins, proteins involved in metabolic processes, protein synthesis and folding, etc. We identified structural proteins such as actin, tubulin and profilin. Profilin could act as pollen allergen as well. This function was described by some authors (Noir etal., 2005; Dai et al., 2006; Sheoran et al., 2007). The identified protein uridine diphosphate (UDP)-glucose 6-dehydrogenase is an enzyme that belongs to the family of oxidoreductases and participates in the biosynthesis of glycosaminoglycans. These glycosylated compounds are common components of the extracellular matrix and likely play roles in signal transduction, metabolism and other cellular processes (Kärkönen et al., 2005; Klinghammer, Tenhaken, 2007). Some identified proteins are involved in metabolic processes, i.e. triose phosphate isomerase is involved in several metabolic pathways including glycolysis (Chen, Thelen, 2010), fructokinase is playing role in sucrose and fructose metabolism. Few proteins participating in protein synthesis and folding were identified, i.e. ribosomal proteins, chaperonin CPN60 and others.

In conclusion, we found that the proteins identified in pollen differed in quantity between the three clover species: red clover cv. 'Vyčiai', berseem clover cv. 'Faraon' and white clover cv. 'Medūnai'. This could contribute to the understanding of the protein quantitative change associated with pollen germination of different clover species.

Table. The summarized search results (by *UniProt*, *Expacy*) of proteins identified from 2DE gels representing protein maps of pollen from red clover cv. 'Vyčiai', berseem clover cv. 'Faraon' and white clover cv. 'Medūnai'

No.[1]	AC[2]	Entry	Description of protein (protein name)	SC[3] %	TP[4]	DP[5]	Theoretical		Experimental		Fold change		
							Mw kDa	pI	Mw kDa	pI	G1/G2	G1/G3	G2/G3
1	2	3	4	5	6	7	8	9	10	11	12	13	14
1*a*	Q9FI17	ARAE4_ARATH	Putative UDP-arabinose 4-epimerase 4 OS = *Arabidopsis thaliana* GN = At5g44480 PE = 3 SV = 1	13	56	7	48.3	9.08	91	5.2	3.7	10.0	2.7
1*b*	Q8GT21	BEBT_CLABR	Benzyl alcohol O-benzoyltransferase OS = *Clarkia breweri* PE = 1 SV = 1	8	49	4	50.6	6.29					
2	P35480	CH60_BRANA	Chaperonin CPN60, mitochondrial OS = *Brassica napus* PE = 2 SV = 1	17	78	8	62.3	8.37	63	7.7	−4.2	2.4	10.1
3*a*	Q2QS14	UGDH4_ORYSJ	UDP-glucose 6-dehydrogenase 4 OS = *Oryza sativa* subsp. *japonica* GN = UGD4 PE = 2 SV = 1	26	55	10	52.8	5.80	56	7.2	−2.3	−2.1	1.1
3*b*	Q2QS13	UGDH5_ORYSJ	UDP-glucose 6-dehydrogenase 5 OS = *Oryza sativa* subsp. *japonica* GN = UGD5 PE = 2 SV = 1	26	56	10	52.9	5.79					
3*c*	Q9FZE1	UGDH1_ARATH	UDP-glucose 6-dehydrogenase 1 OS = *Arabidopsis thaliana* GN = UGD1 PE = 2 SV = 1	32	56	10	52.9	5.84					
3*d*	Q9LIA8	UGDH2_ARATH	UDP-glucose 6-dehydrogenase 2 OS = *Arabidopsis thaliana* GN = UGD2 PE = 1 SV = 1	13	54	7	53.1	5.69					
3*e*	Q9AUV6	UGDH3_ORYSJ	UDP-glucose 6-dehydrogenase 3 OS = *Oryza sativa* subsp. *japonica* GN = UGD3 PE = 2 SV = 1	21	55	9	52.9	5.79					
3*f*	Q96558	UGDH1_SOYBN	UDP-glucose 6-dehydrogenase 1 OS = *Glycine max* GN = UGD1 PE = 1 SV = 1	14	54	6	52.9	5.74					
4*a*	Q2QS13	UGDH5_ORYSJ	UDP-glucose 6-dehydrogenase 5 OS = *Oryza sativa* subsp. *japonica* GN = UGD5 PE = 2 SV = 1	34	56	12	52.9	5.79	55	7.5	1.6	1.8	1.1
4*b*	Q2QS14	UGDH4_ORYSJ	UDP-glucose 6-dehydrogenase 4 OS = *Oryza sativa* subsp. *japonica* GN = UGD4 PE = 2 SV = 1	30	55	11	52.8	5.80					
4*c*	Q9AUV6	UGDH3_ORYSJ	UDP-glucose 6-dehydrogenase 3 OS = *Oryza sativa* subsp. *japonica* GN = UGD3 PE = 2 SV = 1	28	55	11	52.9	5.79					
4*d*	Q9FM01	UGDH4_ARATH	UDP-glucose 6-dehydrogenase 4 OS = *Arabidopsis thaliana* GN = UGD4 PE = 1 SV = 1	22	52	10	53.1	5.60					
4*e*	Q9LIA8	UGDH2_ARATH	UDP-glucose 6-dehydrogenase 2 OS = *Arabidopsis thaliana* GN = UGD2 PE = 1 SV = 1	16	54	8	53.1	5.69					
4*f*	Q96558	UGDH1_SOYBN	UDP-glucose 6-dehydrogenase 1 OS = *Glycine max* GN = UGD1 PE = 1 SV = 1	17	54	7	52.9	5.74					
5	P30171	ACT11_SOLTU	Actin-97 OS = *Solanum tuberosum* GN = AC97 PE = 1 SV = 1	38	39	12	41.6	5.31	45	5.1	1.4	2.0	1.5
6*a*	Q0J6T3	CADH5_ORYSJ	Putative cinnamyl alcohol dehydrogenase 5 OS = *Oryza sativa* subsp. *japonica* GN = CAD5 PE = 3 SV = 2	7	33	3	37.2	6.41	40	6.5	1.9	−1.2	−2.2
6*b*	Q9ZRF1	MTDH_FRAAN	Probable mannitol dehydrogenase OS = *Fragaria ananassa* GN = CAD PE = 1 SV = 1	24	39	5	39.1	6.46					
6*c*	Q6V4H0	10HGO_CATRO	8-hydroxygeraniol dehydrogenase OS = *Catharanthus roseus* GN = 10HGO PE = 1 SV = 1	21	39	6	38.9	6.67					
7	P37706	RRFC_DAUCA	Ribosome-recycling factor, chloroplastic (fragment) OS = *Daucus carota* GN = RRF PE = 2 SV = 2	28	44	9	25.6	9.36	47	10.2	−12.9	−1.6	8.0
8*a*	A2WXV8	SCRK1_ORYSI	Fructokinase-1 OS = *Oryza sativa* subsp. *indica* GN = FRK1 PE = 1 SV = 1	21	36	8	34.7	5.14	34	5.4	1.6	1.4	−1.1
8*b*	Q0JGZ6	SCRK1_ORYSJ	Fructokinase-1 OS = *Oryza sativa* subsp. *japonica* GN = FRK1 PE = 1 SV = 2	17	36	7	34.7	5.07					
8*c*	Q6XZ79	SCRK1_MAIZE	Fructokinase-1 OS = *Zea mays* GN = FRK1 PE = 1 SV = 1	21	34	7	34.7	4.87					
8*d*	Q9M1B9	SCRK4_ARATH	Probable fructokinase-4 OS = *Arabidopsis thaliana* GN = At3g59480 PE = 2 SV = 1	18	36	6	35.0	5.21					
8*e*	Q6XZ78	SCRK2_MAIZE	Fructokinase-2 OS = *Zea mays* GN = FRK2 PE = 1 SV = 1	13	35	6	35.5	5.34					
9*a*	P48497	TPIS_STELP	Triosephosphate isomerase, cytosolic OS = *Stellaria longipes* GN = TPI PE = 1 SV = 1	14	26	3	27.5	5.54	26	6.9	−12.3	−10.1	1.2
9*b*	P48495	TPIS_PETHY	Triosephosphate isomerase, cytosolic OS = *Petunia hybrida* GN = TPIP1 PE = 2 SV = 1	9	27	3	27.1	5.54					
9*c*	P46225	TPIC_SECCE	Triosephosphate isomerase, chloroplastic OS = *Secale cereale* PE = 1 SV = 1	8	32	3	31.6	6.00					
9*d*	P46226	TPIS_SECCE	Triosephosphate isomerase, cytosolic OS = *Secale cereale* PE = 2 SV = 3	9	24	2	26.9	5.24					
9*e*	P12863	TPIS_MAIZE	Triosephosphate isomerase, cytosolic OS = *Zea mays* PE = 3 SV = 3	8	25	2	27.0	5.52					
10*a*	O04905	KCY_ARATH	UMP-CMP kinase OS = *Arabidopsis thaliana* GN = PYR6 PE = 1 SV = 1	14	30	4	22.5	5.79	21	6.9	7.9	3.3	−2.4
10*b*	O24464	KCY_PRUAR	UMP-CMP kinase OS = *Prunus armeniaca* PE = 2 SV = 1	3	30	1	25.9	7.75					
11*a*	O24464	NDK4_SPIOL	Nucleoside diphosphate kinase 4, chloroplastic OS = *Spinacia oleracea* GN = NDK4 PE = 1 SV = 1	20	31	4	25.7	9.15	13	8.2	7.1	−1.1	−7.9
11*b*	P81766	NDK3_SPIOL	Nucleoside diphosphate kinase 3 OS = *Spinacia oleracea* PE = 1 SV = 1	24	22	3	17.1	8.12					

Table continued

1	2	3	4	5	6	7	8	9	10	11	12	13	14
11*c*	O49203	NDK3_ARATH	Nucleoside diphosphate kinase III, chloroplastic/ mitochondrial OS = *Arabidopsis thaliana* GN = NDPK3 PE = 1 SV = 1	12	31	3	25.7	9.28					
11*d*	Q8LAH8	NDK4_ARATH	Nucleoside diphosphate kinase IV, chloroplastic/ mitochondrial OS = *Arabidopsis thaliana* GN = NDK4 PE = 1 SV = 2	12	30	3	25.8	9.44					
12*a*	Q7YJV4	RR18_CALFG	30S ribosomal protein S18, chloroplastic OS = *Calycanthus floridus* var. *glaucus* GN = rps18 PE = 3 SV = 1	46	26	5	11.8	11.96	13	4.2	3.0	−1.4	−4.1
12*b*	Q0G9J7	RR18_LIRTU	30S ribosomal protein S18, chloroplastic OS = *Liriodendron tulipifera* GN = rps18 PE = 3 SV = 1	19	26	5	11.9	11.9					
13	Q84LB6	SUCB_SOLLC	Succinyl-CoA ligase [ADP-forming] subunit beta, mitochondrial OS = *Solanum lycopersicum* PE = 1 SV = 1	28	52	8	44.8	5.86	38	4.2	1.6	1.0	−1.6
14	P80042	GGPPS_CAPAN	Geranylgeranyl pyrophosphate synthase, chloroplastic OS = *Capsicum annuum* GN = GGPS1 PE = 3 SV = 1	23	44	6	40.1	6.12	26	5.1	−1.5	1.8	2.7
15	Q6AUR2	GLNB_ORYSJ	Nitrogen regulatory protein P-II homolog OS = *Oryza sativa* subsp. *japonica* GN = GLB PE = 2 SV = 1	7	30	2	22.7	9.91	25	5.2	−1.8	3.5	6.3
16*a*	P21216	IPYR2_ARATH	Soluble inorganic pyrophosphatase 2 OS = *Arabidopsis thaliana* GN = PPA2 PE = 2 SV = 2	22	29	7	24.7	5.72	26	5.7	1.2	−2.1	−2.5
16*b*	Q949J1	IPYR2_CHLRE	Soluble inorganic pyrophosphatase 2 OS = *Chlamydomonas reinhardtii* GN = ppa2 PE = 1 SV = 1	19	25	5	22.2	5.49					
16*c*	Q0DYB1	IPYR_ORYSJ	Soluble inorganic pyrophosphatase OS = *Oryza sativa* subsp. *japonica* GN = IPP PE = 2 SV = 1	11	27	5	24.1	5.56					
16*d*	Q43187	IPYR_SOLTU	Soluble inorganic pyrophosphatase OS = *Solanum tuberosum* GN = PPA PE = 2 SV = 1	11	28	5	24.2	5.59					
16*e*	O48556	IPYR_MAIZE	Soluble inorganic pyrophosphatase OS = *Zea mays* GN = IPP PE = 2 SV = 1	17	29	5	24.4	5.46					
17	P46745	RT07_PROWI	Ribosomal protein S7, mitochondrial OS = *Prototheca wickerhamii* GN = RPS7 PE = 3 SV = 1	9	38	3	25.2	9.83	26	7.6	−3.2	−1.1	2.9
18	Q5N9Q7	PTHM_ORYSJ	Peptidyl-tRNA hydrolase, mitochondrial OS = *Oryza sativa* subsp. *japonica* GN = Os01g0693900 PE = 2 SV = 1	18	31	5	26.9	10.01	25	8.9	1.6	−2.6	−4.0
19	A4GGE1	YCF2_PHAVU	Protein ycf2 OS = *Phaseolus vulgaris* GN = ycf2-A PE = 3 SV = 1	9	282	15	26.9	8.74	15	8.5	−4.1	−11.8	−2.9
20	Q9TJQ9	RR7_PROWI	30S ribosomal protein S7, plastid OS = *Prototheca wickerhamii* GN = rps7 PE = 3 SV = 1	12	35	2	17.9	10.51	12	7.1	2.2	16.3	7.4
21	A1XFZ5	RK22_NUPAD	50S ribosomal protein L22, chloroplastic OS = *Nuphar advena* GN = rpl22 PE = 3 SV = 1	52	23	8	14.2	10.18	13	4.9	3.3	1.3	−2.6
22*a*	P47922	NDK1_PEA	Nucleoside diphosphate kinase 1 OS = *Pisum sativum* GN = NDPK1 PE = 1 SV = 1	34	17	6	16.5	5.94	14	7.3	1.3	−7.1	−9.5
22*b*	Q39839	NDK1_SOYBN	Nucleoside diphosphate kinase 1 OS = *Glycine max* PE = 1 SV = 1	26	17	4	16.4	5.93					
23*a*	A4GE48	PROBU_OLEEU	Profilin-2 OS = *Olea europaea* PE = 1 SV = 1	28	10	2	14.375	5.06	13	4.5	1.1	4.0	3.5
23*b*	O65812	PROF1_HEVBR	Profilin-1 OS = *Hevea brasiliensis* PE = 1 SV = 1	9	10	1	14.2	4.66					
23*c*	Q8H2C8	PROF2_ARTVU	Profilin-2 OS = *Artemisia vulgaris* PE = 1 SV = 3	8	12	1	14.3	4.79					
23*d*	P0DKE6	PROAB_OLEEU	Profilin-3 OS = *Olea europaea* PE = 1 SV = 1	10	10	1	14.4	5.21					
24*a*	P30171	ACT11_SOLTU	Actin-97 OS = *Solanum tuberosum* GN = AC97 PE = 1 SV = 1	58	39	20	41.6	5.31	51	5.4	−1.3	1.7	2.2
24*b*	P53496	ACT11_ARATH	Actin-11 OS = *Arabidopsis thaliana* GN = ACT11 PE = 1 SV = 1	53	38	19	41.6	5.23					
24*c*	O81221	ACT_GOSHI	Actin OS = *Gossypium hirsutum* PE = 3 SV = 1	59	39	21	41.6	5.31					
24*d*	Q05214	ACT1_TOBAC	Actin OS = *Nicotiana tabacum* PE = 3 SV = 1	57	40	19	41.7	5.46					
24*e*	P53504	ACT1_SORBI	Actin-1 OS = *Sorghum bicolor* GN = AC1 PE = 2 SV = 1	55	39	18	41.8	5.44					
24*f*	Q10DV7	ACT1_ORYSJ	Actin-1 OS = *Oryza sativa* subsp. *japonica* GN = ACT1 PE = 2 SV = 1	60	39	16	41.8	5.30					
25*a*	Q8H8T0	RGP1_ORYSJ	UDP-arabinopyranose mutase 1 OS = *Oryza sativa* subsp. *japonica* GN = UAM1 PE = 1 SV = 1	15	41	6	41.3	5.82	36	6.2	1.0	4.5	4.4
25*b*	Q9FFD2	RGP5_ARATH	Probable UDP-arabinopyranose mutase 5 OS = *Arabidopsis thaliana* GN = RGP5 PE = 1 SV = 1	15	37	5	38.6	5.06					
25*c*	Q9SRT9	RGP1_ARATH	UDP-arabinopyranose mutase 1 OS = *Arabidopsis thaliana* GN = RGP1 PE = 1 SV = 1	21	39	6	40.6	5.61					
25*d*	Q7FAY6	RGP2_ORYSJ	Probable UDP-arabinopyranose mutase 2 OS = *Oryza sativa* subsp. *japonica* GN = UAM2 PE = 1 SV = 1	19	40	5	38.9	6.02					
25*e*	Q9LFW1	RGP2_ARATH	UDP-arabinopyranose mutase 2 OS = *Arabidopsis thaliana* GN = RGP2 PE = 1 SV = 1	17	40	5	40.9	5.76					
25*f*	P80607	UPTG_MAIZE	Alpha-1,4-glucan-protein synthase [UDP-forming] OS = *Zea mays* GN = UPTG PE = 1 SV = 2	12	39	4	41.2	5.75					
25*g*	O04300	UPTG_PEA	Alpha-1,4-glucan-protein synthase [UDP-forming] OS = *Pisum sativum* GN = UPTG PE = 1 SV = 1	12	40	4	41.5	5.73					

Table continued

1	2	3	4	5	6	7	8	9	10	11	12	13	14
26	Q9ZVF2	ML329_ARATH	MLP-like protein 329 OS = *Arabidopsis thaliana* GN = MLP329 PE = 2 SV = 1	50	20	7	17.6	5.30	23	4.2	−1.3	−2.6	−2.0
27*a*	P33629	TBA_PRUDU	Tubulin alpha chain OS = *Prunus dulcis* GN = TUBA PE = 2 SV = 1	44	41	14	49.5	4.92	50	5.1	−1.3	1.5	1.9
27*b*	P46259	TBA1_PEA	Tubulin alpha-1 chain OS = *Pisum sativum* GN = TUBA1 PE = 1 SV = 1	44	41	14	49.6	4.92					
27*c*	Q6VAG0	TBA2_GOSHI	Tubulin alpha-2 chain OS = *Gossypium hirsutum* PE = 2 SV = 1	39	41	13	49.5	4.93					
27*d*	Q6VAF9	TBA4_GOSHI	Tubulin alpha-4 chain OS = *Gossypium hirsutum* PE = 2 SV = 1	42	41	13	49.5	4.93					
27*e*	Q9ZRB7	TBA_WHEAT	Tubulin alpha chain OS = *Triticum aestivum* GN = TUBA PE = 2 SV = 1		41	12	49.7	4.89					
27*f*	Q9ZRR5	TBA3_HORVU	Tubulin alpha-3 chain OS = *Hordeum vulgare* GN = TUBA3 PE = 2 SV = 1	27	41	8	49.7	4.89					
27*g*	P14640	TBA1_MAIZE	Tubulin alpha-1 chain OS = *Zea mays* GN = TUBA1 PE = 3 SV = 1	17	41	7	49.7	4.89					
28*a*	P42054	VDAC_PEA	Outer plastidial membrane protein porin OS = *Pisum sativum* GN = POR1 PE = 1 SV = 2	31	32	8	29.6	9.11	28	10.1	−1.0	−3.3	−3.2
28*b*	P42055	VDAC1_SOLTU	Mitochondrial outer membrane protein porin of 34 kDa OS = *Solanum tuberosum* PE = 1 SV = 2	9	29	3	29.6	8.68					
28*c*	Q6K548	VDAC1_ORYSJ	Mitochondrial outer membrane protein porin 1 OS = *Oryza sativa* subsp. *japonica* GN = VDAC1 PE = 1 SV = 3	4	26	1	29.2	7.07					
28*d*	P42056	VDAC2_SOLTU	Mitochondrial outer membrane protein porin of 36 kDa OS = *Solanum tuberosum* PE = 1 SV = 2	4	27	1	29.4	7.78					
29	Q39434	RB2BV_BETVU	Ras-related protein Rab2BV OS = *Beta vulgaris* GN = RAB2BV PE = 2 SV = 1	2	27	1	23.8	6.44	24	6.1	3.2	−1.1	−3.4
30	Q9SX33	ALA9_ARATH	Putative phospholipid-transporting ATPase 9 OS = *Arabidopsis thaliana* GN = ALA9 PE = 3 SV = 1	1	136	2	13.6	5.91	14	9.5	−3.0	5.8	17.4
31	O48881	TPS1_BRANA	Thiamine biosynthetic bifunctional enzyme BTH1, chloroplastic OS = *Brassica napus* GN = BTH1 PE = 1 SV = 1	2	59	1	56.0	7.15	21	5.5	−1.8	1.7	3.1
32*a*	Q9SRT9	RGP1_ARATH	UDP-arabinopyranose mutase 1 OS = *Arabidopsis thaliana* GN = RGP1 PE = 1 SV = 1	26	39	6	40.6	5.61	38	6.2	−1.3	7.1	9.5
32*b*	Q9LFW1	RGP2_ARATH	UDP-arabinopyranose mutase 2 OS = *Arabidopsis thaliana* GN = RGP2 PE = 1 SV = 1	12	40	4	40.9	5.76					

Notes. Proteins in Figure 2 marked by arrows were analysed and identified by MALDI-TOF MS/MS. Some protein spots represented 2–7 different identified proteins. In the Table they are marked by *a-g*. An increase of spot intensity yields a positive fold-change and a decrease, accordingly a negative fold-change. [1] – spot number, [2] – accession number, [3] – matching (sequence coverage, %), [4] – theoretical peptides, [5] – digest peptides.

Conclusion

Comprehensive proteomic analysis of red clover cv. 'Vyčiai', berseem clover cv. 'Faraon' and white clover cv. 'Medūnai' was performed, more than 200 protein spots in each proteome map representing analysed clover pollen were visualised. Over 30 proteins were identified by using mass spectrometry analysis. Computer-assisted methods were adjusted for evaluation of increase/decrease of the levels of these proteins in analyzed clover pollen protein maps. The identified proteins are involved in different cellular processes – structural and signalling proteins, proteins involved in metabolic processes, protein synthesis and folding, and others. To our knowledge, this proteomic study is the first comprehensive analysis of the protein profiles characteristic of pollen of red clover cv. 'Vyčiai', berseem clover cv. 'Faraon' and white clover cv. 'Medūnai'.

Acknowledgements

This research was funded by a grant (No. SVE-01/2012) from the Research Council of Lithuania. Postdoctoral fellowship (Dr. D. Matuzevičius) is being funded by European Union Structural Funds project "Postdoctoral Fellowship Implementation in Lithuania".

Received 09 01 2014
Accepted 08 07 2014

References

Badr A., El-Shazly, H. H., Watson L. E. 2008. Origin and ancestry of Egyptian clover (*Trifolium alexandrinum* L.) As revealed by AFLP markers. Genetic Resource and Crop Evolution, 55: 21–31 http://dx.doi.org/10.1007/s10722-007-9210-0

Bookstein F. L. 1989. Principal warps: thin plate splines and the decomposition of deformations. IEEE Transactions on Pattern Analysis Machine Intelligence, 11 (6): 567–585 http://dx.doi.org/10.1109/34.24792

Chen M., Thelen J. J. 2010. The plastid isoform of triose phosphate isomerase is required for the postgerminative transition from heterotrophic to autotrophic growth in *Arabidopsis*. The Plant Cell, 22 (1): 77–90 http://dx.doi.org/10.1105/tpc.109.071837

Croner L. J., Kaplan E. 1995. Receptive fields of P and M ganglion cells across the primate retina. Vision Research, 35 (1): 7–24 http://dx.doi.org/10.1016/0042-6989(94)E0066-T

Dai S., Li L., Chen T., Chong K., Xue Y., Wang T. 2006. Proteomic analysis of *Oryza sativa* mature pollen reveal novel proteins associated with pollen germination and tube growth. Proteomics, 6: 2504–2529 http://dx.doi.org/10.1002/pmic.200401351

Dowsey A. W., English J. A., Lisacek F., Morris J. S., Yang G. Z., Dunn M. J. 2010. Image analysis tools and emerging algorithms for expression proteomics. Proteomics, 10 (23): 4226–4257 http://dx.doi.org/10.1002/pmic.200900635

Ellison N. W., Liston A., Steiner J. J., Williams W. M., Taylor N. L. 2006. Molecular phylogenetics of the clover genus (*Trifolium*-Leguminosae). Molecular Phylogenetics and Evolution, l39: 688–705 http://dx.doi.org/10.1016/j.ympev.2006.01.004

Filla J., Capkova V., Fecikova J., Honys D. 2011. Impact of homogenization and protein extraction conditions on the obtained tobacco pollen proteomic patterns. Biologia Plantarum, 55 (3): 499–506 http://dx.doi.org/10.1007/s10535-011-0116-5

Griffiths A. G., Barrett B. A., Simon D., Khan A. K., Bickerstaff P., Anderson C. B., Franzmayr B. K., Hancock K. R., Jones C. S. 2013. An integrated genetic linkage map for white clover (*Trifolium repens* L.) with alignment to Medicago. BMC Genomics, 14: 388–405 http://dx.doi.org/10.1186/1471-2164-14-388

Jevtic G., Andelkovic B., Lugic L., Nedic N., Matovic K. 2013. Colony strength in the spring inspection and its impact on the amount of foraged pollen at the time of red clover pollination. Biotechnology in Animal Husbandary, 29 (1): 115–122 http://dx.doi.org/10.2298/BAH1301115J

Kärkönen A., Murigneux A., Martinant J. P., Pepey E., Tatout C., Dudley B. J., Fry S. C. 2005. UDP-glucose dehydrogenases of maize: a role in cell wall pentose biosynthesis. Biochemical Journal, 391 (2): 409–415 http://dx.doi.org/10.1042/BJ20050800

Klinghammer M., Tenhaken R. 2007. Genome-wide analysis of the UDP-glucose dehydrogenase gene family in *Arabidopsis*, a key enzyme for matrix polysaccharides in cell walls. Journal of Experimental Botany, 58 (13): 3609–3621 http://dx.doi.org/10.1093/jxb/erm209

Lowe D. 2004. Distinctive image features from scale-invariant keypoints. International Journal of Computer Vision, 60 (2): 91–110 http://dx.doi.org/10.1023/B:VISI.0000029664.99615.94

Matuzevicius D. 2010. Analysis of 2D electrophoresis gel images using intelligent techniques: doctoral thesis, Vilnius Gediminas Technical University. Vilnius, Lithuania

Matuzevicius D., Zurauskas E., Navakauskiene R., Navakauskas D. 2008. Improved proteomic characterization of human myocardium and heart conduction system by computational methods. Biologija, 54 (4): 283–289 http://dx.doi.org/10.2478/v10054-008-0058-9

Moller B., Posch S. 2009. Robust features for 2-DE gel image registration. Electrophoresis, 30: 4137–4148 http://dx.doi.org/10.1002/elps.200900293

Noir S., Brautigam A., Colby T., Schmidt J., Pastruga R. 2005. A reference map of the *Arabidopsis thaliana* mature pollen proteome. Biochemical and Biophysical Research Communications, 337: 1257–1266 http://dx.doi.org/10.1016/j.bbrc.2005.09.185

Serackis A., Navakauskas D. 2010. Treatment of over-saturated protein spots in two-dimensional electrophoresis gel images. Informatica, 21 (3): 409–424

Sheoran I. S., Ross A. R. S., Olson D. J. H., Sawhney V. K. 2007. Proteomic analysis of tomato (*Lycopersicon esculentum*) pollen. Journal of Experimental Botany, 58 (13): 3525–3535 http://dx.doi.org/10.1093/jxb/erm199

Sheoran I. S., Ross A. R., Olson D. J., Sawhney V. K. 2009. Differential expression of proteins in the wild type and 7B-1 male-sterile mutant anthers of tomato (*Solanum lycopersicum*): a proteomic analysis. Journal of Proteomics, 71 (6): 624–636 http://dx.doi.org/10.1016/j.jprot.2008.10.006

Shevchenko A., Wilm M., Vorm O., Mann M. 1996. Mass spectrometric sequencing of proteins silver-stained polyacrylamide gels. Analytical Chemistry, 68 (5): 850–858 http://dx.doi.org/10.1021/ac950914h

Vilčinskas E., Dabkevičienė G. 2009. Qualitative and quantitative characteristics of clover (*Trifolium* spp.) species in the first year of growing. Zemdirbyste-Agriculture, 96 (4): 170–180 (in Lithuanian)

Vincent L., Soille P. 1991. Watersheds in digital spaces: an efficient algorithm based on immersion simulations. IEEE Transactions on Pattern Analysis Machine Intelligence, 13 (6): 583–598 http://dx.doi.org/10.1109/34.87344

Williams W. M., Nichols S. N. 2011. *Trifolium*. Kole Ch. (ed.). Wild crop relatives: genomic and breeding resources, legume crops and forages, p. 249–272

Wilson K. A., McManus M. T., Gordon M. E., Jordan T. W. 2002. The proteomics of senescence in leaves of white clover, *Trifolium repens* (L.). Proteomics, 2 (9): 1114–1122 http://dx.doi.org/10.1002/1615-9861(200209)2:9<1114::AID-PROT1114>3.0.CO;2-O

Zhu Y., Zhao P., Wu X., Wang W., Scali M., Cresti M. 2011. Proteomic identification of differentially expressed proteins in mature and germinated maize pollen. Acta Physiologica Plantarum, 33: 1467–1474 http://dx.doi.org/10.1007/s11738-010-0683-7

ISSN 1392-3196 / e-ISSN 2335-8947
Zemdirbyste-Agriculture, vol. 101, No. 4 (2014), p. 453−460
DOI 10.13080/z-a.2014.101.058

Raudonųjų, egiptinių ir baltųjų dobilų žiedadulkių lyginamoji proteominė analizė

G. Treigytė[1], I. Zaikova[1], D. Matuzevičius[2], V. Čeksterytė[3], G. Dabkevičienė[3], B. Kurtinaitienė[1], R. Navakauskienė[1]

[1]Vilniaus universiteto Biochemijos institutas
[2]Vilniaus Gedimino technikos universitetas
[3]Lietuvos agrarinių ir miškų mokslų centro Žemdirbystės institutas

Santrauka

Dobilų, kaip ir daugelio kitų augalų, žiedadulkių proteomo (bendrojo baltymo) struktūriniai komponentai nėra visiškai ištyrinėti. Tyrimo metu atlikta proteomo išsami lyginamoji analizė skirtingų rūšių dobilų – raudonųjų, egiptinių ir baltųjų – žiedadulkėse, surinktose rankomis. Baltymai, išskirti iš veislių ‘Kiršiniai’ bei ‘Vyčiai’ raudonųjų, veislės ‘Faraon’ egiptinių ir veislės ‘Medūnai’ baltųjų dobilų, populiacijų Nr. 2295 4n ir Nr. 2196 4n, buvo frakcionuoti elektroforetiškai pagal molekulinę masę. Nustatytos baltymų grupės, kurios pagal kiekybinį vaizdą skiriasi žiedadulkėse, surinktose iš skirtingų rūšių dobilų. Išsamiajai proteominei analizei pasirinktos veislės ‘Vyčiai’ raudonųjų, veislės ‘Faraon’ egiptinių ir veislės ‘Medūnai’ baltųjų dobilų žiedadulkės. Baltymai, išskirti iš šių žiedadulkių, frakcionuoti dvimatėje baltymų skirstymo sistemoje (2DE) ir vizualizuoti naudojant koloidinio Kumasi mėlio dažą. Kiekviename iš gautų vaizdų identifikuota daugiau kaip 200 baltymų dėmelių. Taikant masių spektrometrinę analizę, identifikuota daugiau nei 30 baltymų. Pritaikius skaitinius metodus, buvo apibūdinti raudonųjų, egiptinių ir baltųjų dobilų žiedadulkių baltymai. Šio tyrimo metu išplėtoti skaitiniai metodai leido įvertinti identifikuotų baltymų raiškos pakitimus raudonųjų, egiptinių bei baltųjų dobilų žiedadulkių proteomo žemėlapiuose, juos tiksliai apibūdinti nustatant molekulinę masę, izoelektrinį tašką ir įvertinti kiekybinius pakitimus.

Reikšminiai žodžiai: proteominė analizė, *Trifolium alexandrinum*, *T. pratense*, *T. repens,* žiedadulkės.